FULL PAPER

Dalton
www.rsc.org/dalton

Formation of [2 + 2] diruthenium(II) metallomacrocycles from ligands containing 2,2′:6′,2″-terpyridine domains linked through flexible polyethyleneoxy spacers†

Edwin C. Constable,* Catherine E. Housecroft,* Markus Neuburger, Silvia Schaffner and Christopher B. Smith*‡

Department of Chemistry, University of Basel, Spitalstrasse 51, CH-4056, Basel, Switzerland. E-mail: edwin.constable@unibas.ch; Fax: 41 61 267 1018; Tel: 41 61 267 1001

Received 5th April 2005, Accepted 19th May 2005
First published as an Advance Article on the web 9th June 2005

The syntheses of three ligands containing two terpy metal-binding domains linked through flexible polyethyleneoxy spacers are described. These ligands have been utilised as building blocks in a two-step process for the formation of a series of dinuclear ruthenium(II) metallomacrocycles of the type $[Ru_2\mathbf{L}_2]^{4+}$. Employing a two-step methodology allows the formation of homoleptic ($[Ru_2\mathbf{L}_2]^{4+}$) and heteroleptic ($[Ru_2\mathbf{LL}']^{4+}$) species in which the ligands differ in the length of the polyethyleneoxy spacer connecting each terpy motif. Homoleptic metallomacrocycles have been characterised through single crystal X-ray diffraction studies, while 2D-NMR spectroscopy has been employed for the characterisation of the heteroleptic species.

Introduction

Ligands containing multiple terpy metal binding domains show promise as building-blocks for the self-assembly of supramolecular architectures. In particular, studies have centred upon the spontaneous self-assembly of metallomacrocycles[1–7] and metallopolymers[8–12] upon interaction with metal salts. The factors controlling the formation of polymer or cyclic structure are currently unclear. Metallomacrocycles have been studied with a view to applications as catalysts,[13] sensors[14] or receptors[15] or in crystal engineering,[16] with metallocrowns, analogues of crown ethers in which backbone carbon atoms are replaced by metal ions, being of particular interest.[17] The $\{M(terpy)_2\}$ motif is an attractive one for incorporation into metallomacrocycles as it is achiral (if the linkage is through the 4′-position of the central ring) and multinuclear species may be prepared without the complication of formation of diastereoisomers. Prototype metallomacrocycles based upon two terpy metal-binding domains were linked through rigid, preorganised spacers to avoid uncontrolled polymer and oligomer formation and typically utilised labile first row transition metal ions such as iron(II) or cobalt(II) or kinetically inert ruthenium(II) centres in a stepwise self-assembly process.[3] More recently, we have shown that discrete metallomacrocyclic species may be formed in cases where the two terpy domains are separated by spacers of varying degrees of flexibility.[4–7] In this paper, we report the synthesis of four diruthenium(II) metallomacrocycles containing ditopic terpy ligands (Scheme 1) in which the terpy domains are linked through flexible polyethyleneoxy spacers.

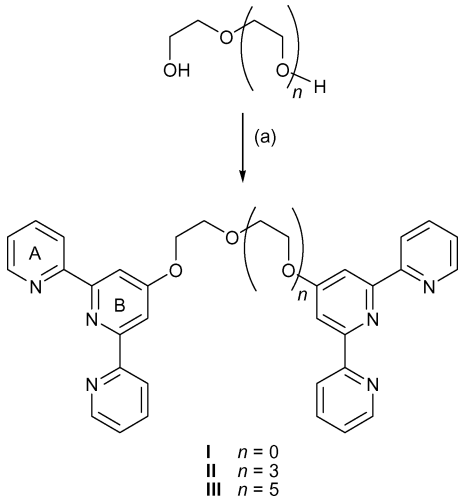

Scheme 1 Ligands presented in this paper. *Reagents*: (a) 4′-chloro-2,2′:6′,2″-terpyridine (Clterpy), KOH, DMSO. Ring labelling is as used in the ^{1}H NMR spectroscopic assignments of the free ligands and homoleptic complexes.

Experimental

General

^{1}H NMR spectra were recorded on Bruker AM 250, AM 300 or DRX 500 MHz spectrometers; ^{13}C NMR spectra were recorded on a Bruker DRX 500 MHz spectrometer operating at 125.76 MHz. UV/VIS measurements were recorded on a Varian Cary 5000 UV-Vis-NIR spectrophotometer in acetonitrile solution. ESMS spectra were recorded on a Finnigan MAT LCQ ESI/MS instrument. Elemental analyses were carried out in the Department of Chemistry, University of Basel. Solvents and reagents were used as received unless otherwise specified. DMSO was dried before use over preactivated 3 Å molecular sieve.[18]

Preparations

1,2-Bis(2,2′:6′,2″-terpyridin-4′-yloxy)ethane, I. 1,2-Ethanediol (35 mg, 0.56 mmol) was added to a suspension of KOH (220 mg 85%, 3.34 mmol) in DMSO (6 cm^3). The suspension was stirred for 1 h at 70 °C after which Clterpy[19] (604 mg, 2.26 mmol) and DMSO (5 cm^3) were added and the mixture heated at 70 °C for 27 h. After cooling to room temperature, the brown mixture was poured into water (100 cm^3) and the milky suspension was extracted with $CHCl_3$ (3 × 50 cm^3) and the extracts washed with water (50 cm^3), dried ($MgSO_4$) and evaporated. The solid residue was purified by column chromatography on alumina gel eluting with $CHCl_3$ (to remove excess Clterpy), followed by

† Electronic supplementary information (ESI) available: ^{1}H NMR spectra of ligands **I**, **II** and **III**, $[Ru_2(\mathbf{II})_2][PF_6]_4$, $[Ru_2(\mathbf{III})_2][PF_6]_4$, $[Ru_2(\mathbf{I})(\mathbf{III})][PF_6]_4$ and $[Ru_2(\mathbf{II})(\mathbf{III})][PF_6]_4$ (Figs. S1–S4). See http://www.rsc.org/suppdata/dt/b5/b504670j/

‡ Current address: School of Biomedical and Chemical Sciences, University of Western Australia, Crawley, Perth, WA 6009, Australia.

DOI: 10.1039/b504670j

$CHCl_3$–MeOH (96 : 4) to afford the pure compound **I** as a white powder. Yield 160 mg, 54%. δ_H/ppm (300 MHz, $CDCl_3$–DMSO-d_6) 8.70 (m, 4H, H_6), 8.63 (d, 4H, H_3), 8.11 (s, 4H, $H_{3'}$), 7.86 (dt, 4H, H_4), 7.34 (m, 4H, H_5), 4.69 (s, 4H, CH_2). *m*/*z* 525 $[MH]^+$ (ESMS).

1,11-Bis(2,2′:6′,2″-terpyridin-4′-yloxy)-3,6,9-trioxaundecane, II. 3,6,9-Trioxaundecane-1,11-diol (200 mg, 1.03 mmol) was added to a suspension of crushed KOH (570 mg 85%, 8.65 mmol) in DMSO (15 cm^3). Clterpy (1.65 g, 6.16 mmol) was added, and the suspension heated at 60 °C for 42 h, after which the reaction was judged to be complete by TLC analysis (alumina, $CHCl_3$–MeOH 94 : 6). The mixture was then poured into water (200 cm^3) and extracted with $CHCl_3$ (4 × 50 cm^3). The organic extracts were combined, washed with water (100 cm^3) and dried (Na_2SO_4). Filtration and evaporation gave an off-white solid which was purified by column chromatography ($CHCl_3$–MeOH, 96 : 4) as for **I** to give ligand **II** (600 mg, 89%) as a white powder. δ_H/ppm (250 MHz, $CDCl_3$) 8.68 (m, 4H, H_6), 8.62 (d, 4H, H_3), 8.06 (s, 4H, $H_{3'}$), 7.86 (m, 4H, H_4), 7.34 (m, 4H, H_5), 4.41 (t, 4H, CH_2), 3.93 (t, 4H, CH_2), 3.75 (m, 4H, CH_2), 3.70 (m, 4H, CH_2). Found: C, 69.52; H, 5.43; N, 12.76. $C_{38}H_{36}N_6O_5$ requires C, 69.50; H, 5.53; N, 12.80%. *m*/*z* 679 $[M + Na]^+$ (ESMS).

1,11-Bis(2,2′:6′,2″-terpyridin-4′-yloxy)-3,6,9,12,15-pentaoxaheptadecane, III. 3,6,9,12,15-Pentaoxaheptadecane-1,17-diol (314 mg, 1.11 mmol) and crushed KOH (440 mg 85%, 6.68 mmol) were added to DMSO (15 cm^3) and the mixture stirred for 1 h at 70 °C, after which Clterpy (1.19 g, 4.45 mmol) was added. The suspension was heated at 70 °C for 24 h, then allowed to cool before being poured into water (150 cm^3). The mixture was extracted with $CHCl_3$ (3 × 50 cm^3) and the organic extracts then washed with water (50 cm^3). After drying (Na_2SO_4) and evaporation of solvent, the oily residue was purified by column chromatography over alumina. Excess Clterpy was removed by eluting with $CHCl_3$, followed by $CHCl_3$–MeOH (96 : 4) to give **III** as a colourless oil (581 mg, 70%). δ_H/ppm (250 MHz, $CDCl_3$) 8.65 (m, 4H, H_6), 8.57 (d, 4H, H_3), 8.01 (s, 4H, $H_{3'}$), 7.80 (dt, 4H, H_4), 7.28 (m, 4H, H_5), 4.36 (t, 4H, CH_2), 3.89 (t, 4H, CH_2), 3.72 (m, 4H, CH_2), 3.66 (m, 4H, CH_2), 3.63 (s, 8H, CH_2). *m*/*z* 768 $[M + Na]^+$ (ESMS).

$[Cl_3Ru(I)RuCl_3]$. A suspension of **I** (102 mg, 0.194 mmol) and "$RuCl_3 \cdot 3H_2O$" (101 mg, 0.386 mmol) was heated to reflux in ethanol (50 cm^3) for 3 h The ligand dissolved over this period and a brown precipitate was deposited. After cooling to room temperature, the precipitated solid was collected by filtration and washed with ethanol (10 cm^3) to give $[Cl_3Ru(\mathbf{I})RuCl_3]$ which was used without further purification. Yield 148 mg, 81%.

$[Cl_3Ru(II)RuCl_3]$. This complex was prepared in an analogous procedure to that described for $[Cl_3Ru(\mathbf{I})RuCl_3]$ from **II** (103 mg, 0.156 mmol) and "$RuCl_3 \cdot 3H_2O$" (82 mg, 0.313 mmol) in EtOH (50 cm^3). $[Cl_3Ru(\mathbf{II})RuCl_3]$ was obtained as a brown powder in 95% yield and used without further purification (159 mg).

$[Cl_3Ru(III)RuCl_3]$. This compound was prepared in an analogous manner to $[Cl_3Ru(\mathbf{I})RuCl_3]$ using **III** (127 mg, 0.170 mmol) and $RuCl_3 \cdot 3H_2O$ (89 mg, 0.34 mmol) in EtOH (40 cm^3). The complex $[Cl_3Ru(\mathbf{III})RuCl_3]$ was obtained as a brown powder in 95% yield and used without further purification (141 mg).

$[Ru_2(II)_2][PF_6]_4$. A mixture of $[Cl_3Ru(\mathbf{II})RuCl_3]$ (35.2 mg, 0.0329 mmol), **II** (21.6 mg, 0.0329 mmol) and *N*-ethylmorpholine (10 drops) was heated to reflux in MeOH (40 cm^3). The suspended solid had dissolved after 30 min, and over time the solution turned dark red. After 30 min, TLC analysis (silica gel, MeCN–saturated aqueous KNO_3–H_2O, 7 : 1 : 0.5) indicated the presence of a major red component at R_f 0.25 in addition to two minor pink species at higher R_f and some streaky orange baseline material. Heating the reaction mixture overnight did not change the product distribution. The reaction mixture was cooled, filtered through Celite to remove traces of insoluble material, and the solution concentrated *in vacuo* to 10 cm^3, followed by addition of saturated aqueous NH_4PF_6 solution. The red precipitate that resulted was collected by filtration over Celite, washed with water (100 cm^3) and redissolved in MeCN (2 cm^3). The crude product was purified by column chromatography (silica gel, MeCN–saturated aqueous KNO_3–H_2O, 7 : 1 : 0.5), and the major red band was collected. The eluate was concentrated in volume, and the product reprecipitated by addition of aqueous NH_4PF_6 solution. After filtering over Celite and washing with water (100 cm^3) the product was dissolved by the addition of MeCN (20 cm^3). The resultant clear red solution was evaporated to dryness to afford $[Ru_2(\mathbf{II})_2][PF_6]_4$ as a deep red microcrystalline solid (24 mg, 35%). δ_H/ppm (250 MHz, CD_3CN) 8.29 (s, 8H, H_{3B}), 8.26 (d, 8H, H_{3A}), 7.27 (dt, 8H, H_{4A}), 7.24 (m, 8H, H_{6A}), 6.78 (m, 8H, H_{5A}), 4.67 (t, 8H, CH_2), 4.05 (t, 8H, CH_2), 3.81 (m, 8H, CH_2), 3.68 (m, 8H, CH_2). *m*/*z* 1950 $[M - PF_6]^+$, 903 $[M - 2PF_6]^{2+}$ (ESMS). Found: C, 42.30; H, 3.62; N, 7.93. $C_{76}H_{72}F_{24}N_{12}O_{10}P_4Ru_2 \cdot 3H_2O$ requires C, 42.47; H, 3.66; N, 7.82%. λ_{max}/nm (CH_3CN) 243 (ε/dm^3 mol^{-1} cm^{-1} 73100), 265 (76500), 305 (92300), 483 (25700, MLCT). R_f 0.25 (silica gel, MeCN–saturated aqueous KNO_3–H_2O, 7 : 1 : 0.5).

$[Ru_2(III)_2][PF_6]_4$. $[Cl_3Ru(\mathbf{III})RuCl_3]$ (56 mg, 0.0483 mmol) and **III** (36 mg, 0.0483 mmol) were heated to reflux in MeOH (50 cm^3) containing *N*-ethylmorpholine (10 drops). The reaction was monitored by TLC (silica gel, MeCN–saturated aqueous KNO_3–H_2O, 7 : 1 : 0.5) and showed no further changes after 3 h. After cooling to room temperature the reaction was worked up as described for $[Ru_2(\mathbf{II})_2][PF_6]_4$ to afford $[Ru_2(\mathbf{III})_2][PF_6]_4$ as a red solid. Yield 35 mg, 32%. δ_H/ppm (250 MHz, CD_3CN) 8.37 (d, 8H, H_{3A}), 8.29 (s, 8H, H_{3B}), 7.69 (dt, 8H, H_{4A}), 7.32 (m, 8H, H_{6A}), 6.95 (m, 8H, H_{5A}), 4.62 (m, 8H, CH_2), 4.01 (m, 8H, CH_2), 3.76 (m, 8H, CH_2), 3.65 (m, 8H, CH_2), 3.61 (s, 16H, CH_2). *m*/*z* 991 $[M - 2PF_6]^{2+}$, 598 $[(HOterpy)Ru(terpyO)]^+$, 300 $[Ru(HOterpy)_2]^{2+}$ (ESMS). Found: C, 43.63; H, 3.93; N, 7.57. $C_{84}H_{88}F_{24}N_{12}O_{14}P_4Ru_2 \cdot 2H_2O$ requires C, 43.72; H, 4.02; N, 7.28%. λ_{max}/nm (CH_3CN) 242 (ε/dm^3 mol^{-1} cm^{-1} 122600), 266 (128300), 304 (156400), 486 (44200, MLCT). R_f 0.5 (silica gel, MeCN–saturated aqueous KNO_3–H_2O, 7 : 1 : 0.5).

$[Ru_2(I)(III)][PF_6]_4$. Ligand **III** (45.0 mg, 0.604 mmol) and $[Cl_3Ru(\mathbf{I})RuCl_3]$ (56.7 mg, 6.03 mmol) were heated under reflux with *N*-ethylmorpholine (10 drops) in MeOH (40 cm^3). After 1 h the reactants had dissolved and were replaced with a fine red solid and a deep red solution. After heating overnight, the suspension was cooled, and the solid material filtered off. The red filtrate was concentrated in volume and saturated aqueous NH_4PF_6 solution was added to precipitate the crude product. This material was purified as for $[Ru_2(\mathbf{II})_2][PF_6]_4$ and the major red fraction was treated with NH_4PF_6 solution to give $[Ru_2(\mathbf{I})(\mathbf{III})][PF_6]_4$ as a red solid (16 mg, 13%). δ_H/ppm (500 MHz, CD_3CN) 8.36 (d, 4H, H_{3C}), 8.35 (s, 4H, H_{3D}), 8.28 (s, 4H, H_{3B}), 7.89 (d, 4H, H_{3A}), 7.64 (dt, 4H, H_{4C}), 7.35 (m, 4H, H_{6C}), 7.29 (m, 4H, H_{4A}), 7.28 (m, 4H, H_{6A}), 6.99 (m, 4H, H_{5A}), 6.85 (m, 4H, H_{5C}), 5.25 (s, 4H, CH_2), 4.72 (m, 4H, CH_2), 3.99 (m, 4H, CH_2), 3.69 (m, 4H, CH_2), 3.56 (m, 4H, CH_2), 3.47 (s, 8H, CH_2). δ_C/ppm (125 MHz, CD_3CN) 166.24, 165.27, 158.39, 157.75, 156.24, 156.17, 152.70, 152.02, 137.74, 137.37, 127.60, 127.18, 112.01, 111.76, 70.42, 70.11, 69.96, 69.78, 69.67, 69.61, 68.75. *m*/*z* 1907 $[M - PF_6]^+$, 881 $[M - 2PF_6]^{2+}$, 736 $\{[(terpy)Ru(\mathbf{III})Ru][PF_6]_2\}^{2+}$, 598 $[(HOterpy)Ru(terpyO)]^+$ (ESMS). Found: C, 41.58; H, 3.63; N, 7.58. $C_{74}H_{68}N_{12}F_{24}O_9P_4Ru_2 \cdot 5H_2O$ requires C, 41.50; H, 3.67; N, 7.85%. λ_{max}/nm (CH_3CN) 243 (ε/dm^3 mol^{-1} cm^{-1} 75200), 267 (78500), 305 (93200), 485 (26800, MLCT). R_f 0.4 (silica gel, MeCN–saturated aqueous KNO_3–H_2O, 7 : 1 : 0.5).

$[Ru_2(II)(III)][PF_6]_4$. Ligand **II** (19.7 mg, 0.0300 mmol) and $[Cl_3Ru(\mathbf{III})RuCl_3]$ (34.8 mg, 0.0300 mmol) were heated to reflux

in MeOH (40 cm^3) containing *N*-ethylmorpholine (10 drops). The solid reactants dissolved over time to give a deep red solution. After 2 h, TLC analysis (silica gel, MeCN–saturated aqueous KNO_3–H_2O, 7 : 1 : 0.5) after 2 h showed the presence of a major red mobile species at R_f 0.4, in addition to some streaky material on the baseline. After heating overnight, the reaction mixture was worked up as described for $[Ru_2(\mathbf{II})_2][PF_6]_4$. The major red fraction was collected and the product precipitated as the solid red hexafluorophosphate salt. Yield of 29 mg, 45%. δ_H/ppm (500 MHz, CD_3CN) 8.32 (d, 4H, H_{3C}), 8.29 (d, 4H, H_{3A}), 8.283 (s, 4H, H_{3B} or H_{3D}), 8.277 (s, 4H, H_{3B} or H_{3D}), 7.52 (dt, 4H, H_{4C}), 7.32 (dt, 4H, H_{4A}), 7.31 (m, 4H, H_{6A}), 7.17 (m, 4H, H_{6C}), 6.98 (m, 4H, H_{5C}), 6.47 (m, 4H, H_{5A}), 4.64 (m, 8H, CH_2), 4.02 (m, 8H, CH_2), 3.79 (m, 4H, CH_2), 3.76 (m, 4H, CH_2), 3.70 (m, 4H, CH_2), 3.66 (m, 4H, CH_2), 3.62 (s, 8H, CH_2). δ_C/ppm (125 MHz, CD_3CN) 165.82, 165.69, 158.16, 158.09, 156.24, 156.22, 152.42, 152.32, 137.48, 137.19, 127.34, 126.84, 124.26, 124.20, 111.04, 110.96, 70.71, 70.56, 70.37, 70.20, 70.10 (2), 69.81, 69.75, 68.84, 68.80. *m/z* 947 $[M - 2PF_6]^{2+}$, 598 $[(HOterpy)Ru(terpyO)]^+$, 300 $[Ru(HOterpy)_2]^{2+}$ (ESMS). Found: C, 41.54; H, 3.66; N, 7.31. $C_{80}H_{80}N_{12}F_{24}O_{12}P_4Ru_2{\cdot}6H_2O$ requires C, 41.93; H, 4.05; N, 7.33%. λ_{max}/nm (CH_3CN) 243 (ε/dm^3 mol^{-1} cm^{-1} 65700), 266 (70000), 305 (87100), 486 (25100, MLCT). R_f 0.4 (silica gel, MeCN–saturated aqueous KNO_3–H_2O, 7 : 1 : 0.5).

Crystal structure determinations

Data were collected on an Enraf Nonius Kappa CCD instrument; data reduction, solution and refinement used the programs COLLECT,[20] SIR92[21] and CRYSTALS.[22]

Crystal data for $[Ru_2(\mathbf{II})_2][PF_6]_4{\cdot}6MeCN$. $C_{88}H_{90}F_{24}N_{18}O_{10}P_4Ru_2$, $M = 2338.76$, triclinic, space group $P\bar{1}$, $a = 13.746(1)$, $b = 14.810(4)$, $c = 15.067(3)$ Å, $\alpha = 100.87(2)$, $\beta = 111.407(9)$, $\gamma = 111.29(2)°$, $U = 2471.8(12)$ Å^3, $Z = 1$, $D_c = 1.571$ Mg m^{-3}, μ(Mo-Kα) = 0.481 mm^{-1}, $T = 173$ K, 11329 reflections collected on an Enraf Nonius Kappa CCD instrument. Refinement of 7167 reflections (737 parameters) with $I > 2.0\sigma(I)$ converged at final $R1 = 0.0598$, $wR2 = 0.0536$, GOF = 1.06.

Crystal data for $[Ru_2(\mathbf{III})_2][PF_6]_4{\cdot}2H_2O{\cdot}MeCN$. $C_{86}H_{91}F_{24}N_{13}O_{16}P_4Ru_2$, $M = 2344.74$, triclinic, space group $P\bar{1}$, $a = 8.360(8)$, $b = 15.497(9)$, $c = 20.71(1)$ Å, $\alpha = 73.44(4)$, $\beta = 84.71(8)$, $\gamma = 83.69(8)°$, $U = 2551(3)$ Å^3, $Z = 1$, $D_c = 1.526$ Mg m^{-3}, μ(Mo-Kα) = 0.469 mm^{-1}, $T = 173$ K, 11417 reflections collected on an Enraf Nonius Kappa CCD instrument. Refinement of 7448 reflections (740 parameters) with $I > 2.0\sigma(I)$ converged at final $R1 = 0.1092$, $wR2 = 0.1010$, GOF = 1.01.

CCDC reference numbers 253694 and 267866.

See http://www.rsc.org/suppdata/dt/b5/b504670j/ for crystallographic data in CIF or other electronic format.

Results and discussion

Ligand synthesis and characterisation

The target ligands have two 4′-functionalised terpy metal-binding domains linked by polyethyleneoxy chains of various lengths. The polyethyleneoxy spacer was chosen to give a reasonable degree of flexibility, but also because there will be a degree of preorganisation associated with the helical coiling which could potentially be addressed with Group 1 and 2 metal ions. Two strategies are possible for ligands **I–III**; firstly, nucleophilic 4′-hydroxy-2,2′:6′,2″-terpyridine could be reacted with polyethyleneoxy chlorides, tosylates or mesylates and, secondly, Clterpy could be reacted with the (poly)ethyleneglycols under basic conditions. We favoured the latter approach as it did not necessitate the use of the electrophilic oxygen mustards.

The homoditopic ligands **I**, **II** and **III** were readily prepared using standard methodology by reacting the appropriate nucleophilic diol with an excess of the electrophile 4′-chloro-2,2′:6′,2″-terpyridine (Clterpy)[19] in DMSO in the presence of KOH (Scheme 1).[4–6,23,24] After purification by chromatography, the ligands were obtained in good yields as white solids, or in the case of **III** a colourless oil, and with analytical purity. The ^{1}H NMR spectrum of each ligand shows the expected pattern for 4′-substituted terpy compounds, and confirms that the terpy domains in each ligand are equivalent and symmetrical with the two A rings being equivalent. All proton signals are well resolved. In the ^{1}H NMR spectra of the three ligands, the major differences lie in the signals attributable to the spacer units. In **I**, both sets of methylene signals are observed as a singlet, while in **II** and **III**, the sets of chemically and magnetically non-equivalent methylene protons are present at distinctly different chemical shifts. The ligands were also characterised by electrospray mass spectrometry. Spectra for **I** and **II** exhibited peaks at *m/z* 525 and 679 assigned to $[MH^+]$ and $[M + Na]^+$, respectively. The spectrum for **III** showed a base peak at *m/z* 768 assigned to $[M + Na]^+$. Satisfactory elemental analysis results confirmed the purity of **I** and **II**. Compound **III** is a viscous oil and could not be obtained completely free of solvent for analysis.

Metallomacrocycle formation: methodology

We envisaged that metallomacrocycles could be formed from ligands **I**, **II** and **III** using a two-step methodology. The first step involves reacting the ligand with two equivalents of ruthenium trichloride in ethanol to form an isolable, dinuclear ruthenium(III) complex $[Cl_3Ru(\mathbf{L})RuCl_3]$ (**L** = **I**, **II** or **III**). Reaction of this complex with an equimolar amount of **I**, **II** or **III** under conditions of medium-to-high dilution in the presence of a reducing agent (*N*-ethylmorpholine) could afford ruthenium(II) metallomacrocycles or metallopolymers which can be isolated as their hexafluorophosphate salts. In all cases, the only isolable metallomacrocyclic products were dinuclear complexes and the general strategy for their formation is shown in Scheme 2.

This two-step methodology to form complexes containing $[Ru(terpy)_2]^{2+}$ motifs has been widely used,[25] and has been employed recently by Newkome and coworkers for the synthesis of [6 + 6] ruthenium(II) metallomacrocycles.[3] The formation of these hexagonal metallomacrocycles by this method was particularly efficient as a result of the terpy motifs being positioned between rigid, short spacer regions at the correct internal angle for the formation of a regular hexagon (120°).[3] The formation of metallomacrocycles using ligands **I–III** was more speculative owing to the flexible nature of the spacers in these systems. As a consequence, conditions of medium-to-high dilution were utilised to minimise the potential formation of metallopolymers.

Formation of $[Cl_3Ru(L)RuCl_3]$, L = I, II or III

Following the procedure outlined above, ligand **II** was converted to the ruthenium(III) complex $[Cl_3Ru(\mathbf{II})RuCl_3]$ by heating **II** with a stoichiometric amount of ruthenium(III) trichloride in ethanol. This complex was obtained as a brown precipitate in 81% isolated yield and was very insoluble in a most organic solvents. This is a common property of $[Ru(Xterpy)Cl_3]$ complexes,[23–25] and the material was dried and used in the subsequent reactions without further purification or characterization. Ligands **I** and **III** were similarly converted to the analogous complexes $[Cl_3Ru(\mathbf{I})RuCl_3]$ and $[Cl_3Ru(\mathbf{III})RuCl_3]$ and were also used without further purification.

Formation and characterization of $[Ru_2(\mathbf{II})_2][PF_6]_4$ and $[Ru_2(\mathbf{III})_2][PF_6]_4$

The complexes $[Cl_3Ru(\mathbf{II})RuCl_3]$ and $[Cl_3Ru(\mathbf{III})RuCl_3]$ were first used in reactions with ligands **II** and **III** respectively as described below, the aim being to investigate the formation of metallocyclic products. In contrast to ligands **II** and **III**, ligand **I** gave only polymeric material in test reactions with labile iron(II)

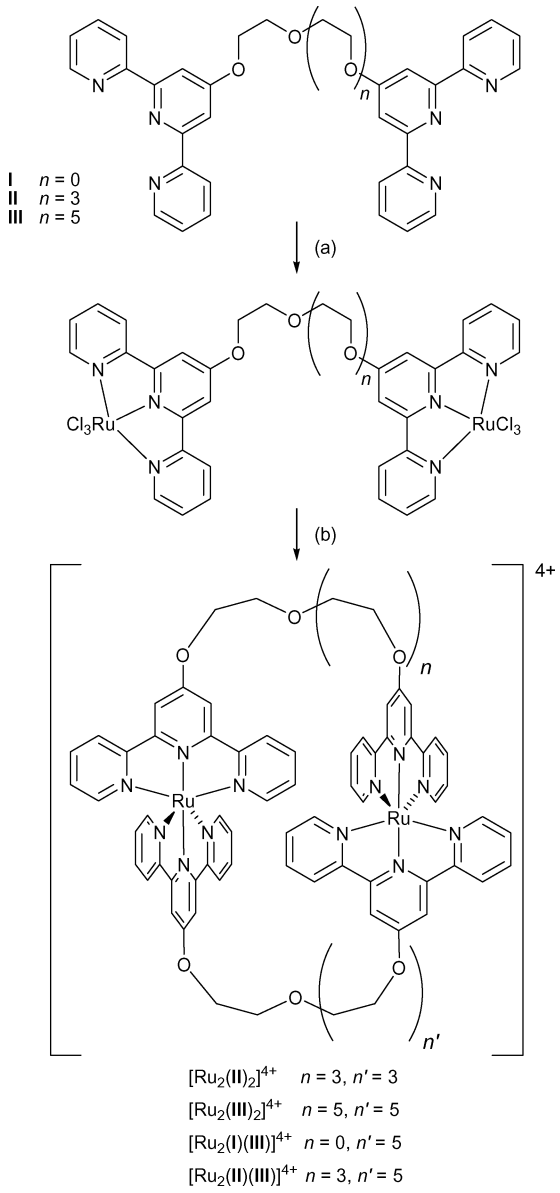

Scheme 2 Synthetic route to the diruthenamacrocyles. *Reagents.* (a) $RuCl_3 \cdot 3H_2O$, EtOH, reflux, 3 h; (b) second ligand, *N*-ethylmorpholine, DMF, reflux.

salts. On the basis of this, we have not yet further investigated reactions of **I** with [Cl_3Ru(**I**)$RuCl_3$].

Ligand **II** and the complex [Cl_3Ru(**II**)$RuCl_3$] were combined in an equimolar ratio in methanol containing *N*-ethylmorpholine as a reducing agent and the mixture heated under reflux. After a short time, the insoluble diruthenium(III) complex began to dissolve and the solution changed colour to deep red, indicating the formation of a $\{Ru(terpy)_2\}^{2+}$ chromophore.[25] Analysis of the solution composition by TLC showed a red product with $R_f = 0.25$ to be the dominant species. Small traces of a pink species at higher R_f and small amounts of an orange immobile material (assumed to be polymeric) were observed. Prolonged reaction times (>24 h) resulted in little change in the product distribution. After concentrating the solution *in vacuo* and adding saturated aqueous NH_4PF_6 solution, a red precipitate was obtained, which was further purified by column chromatography. The major red fraction was collected and reprecipitated with saturated aqueous NH_4PF_6 solution, to give [Ru_2(**II**)$_2$][PF_6]$_4$ as a deep red solid in 35% yield. The complex [Ru_2(**III**)$_2$][PF_6]$_4$ was similarly obtained in 32% yield from the reaction of **III** with [Cl_3Ru(**III**)$RuCl_3$].

The results of electrospray mass spectrometry for the new complexes were consistent with the formation of [2 + 2] ruthenamacrocycles. In the ES mass spectrum of [Ru_2(**II**)$_2$][PF_6]$_4$, the highest mass peak envelopes came at *m*/*z* 1950 and 903 corresponding to $[M - PF_6]^+$ and $[M - 2PF_6]^{2+}$, respectively. These peaks exhibited the correct isotopomer distribution for dinuclear Ru(II) species. In the mass spectrum of [Ru_2(**III**)$_2$][PF_6]$_4$, the highest mass peak was at *m*/*z* 991 and corresponded to $[M - 2PF_6]^{2+}$. Further fragmentation was observed leading to $[(HOterpy)Ru(terpyO)]^+$ (*m*/*z* 598) and $[Ru(HOterpy)_2]^{2+}$ (*m*/*z* 300) with all peak envelopes exhibiting isotopomer patterns matching those simulated.

The ^{1}H NMR spectra of CD_3CN solutions of [Ru_2(**II**)$_2$][PF_6]$_4$ and [Ru_2(**III**)$_2$][PF_6]$_4$ confirm that the complexes are highly symmetrical, with the terminal rings within each terpy subunit, and the two terpy subunits in each ligand, being equivalent. Proton signals were assigned by comparison with other $[Ru(4'\text{-X-terpy})_2]^{2+}$ complexes.

Single crystals of [Ru_2(**II**)$_2$][PF_6]$_4$·6MeCN suitable for X-ray diffraction were grown by diffusion of diethyl ether vapour into an acetonitrile solution of the complex. The structure of the cation is shown in Fig. 1, and selected bond distances and

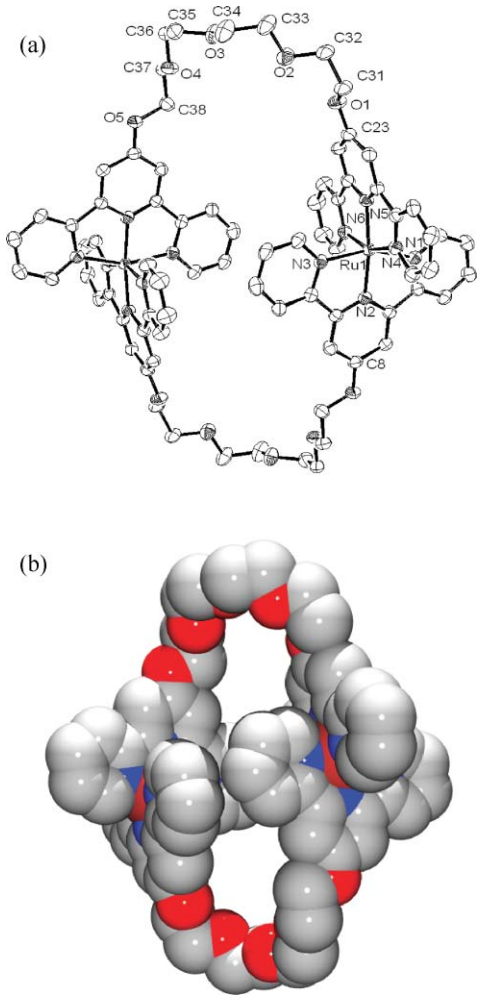

Fig. 1 (a) The molecular structure and atom labelling and (b) a space-filling diagram of the dinuclear cation in [Ru_2(**II**)$_2$][PF_6]$_4$·6MeCN. Hydrogen atoms are omitted for clarity. Atoms in the second half of the molecule are related to the first by inversion through a centre of symmetry. Selected bond lengths (Å) and angles (°): Ru(1)–N(1) 2.063(3), Ru(1)–N(2) 1.972(3), Ru(1)–N(3) 2.055(3), Ru(1)–N(4) 2.080(3), Ru(1)–N(5) 1.978(3), Ru(1)–N(6) 2.059(4), C(23)–O(1) 1.354(5), C(8′)–O(5) 1.348(5); other C–O in the range 1.402(6)–1.444(5); N(1)–Ru(1)–N(2) 78.8(1), N(2)–Ru(1)–N(3) 78.8(1), N(4)–Ru(1)–N(5) 78.6(1), N(5)–Ru(1)–N(6) 79.3(1), C(31)–O(1)–C(23) 116.6(3), C(38)–O(5)–C(8′) 116.3(3), C(32)–O(2)–C(33) 112.1(4), C(34)–O(3)–C(35) 111.9(3), C(36)–O(4)–C(37) 110.3(3).

angles are given in the figure caption. The structure confirms the formation of a [2 + 2] ruthenamacrocyclic complex. In the crystal lattice, the metallomacrocycle lies on a centre-of-symmetry. Each ruthenium(II) centre is coordinated by two terpy domains, one from each ligand **II**. Each metal centre is six-coordinate, with the expected pattern of shorter Ru–N bonds to the central and longer Ru–N bonds to the terminal pyridine rings. Bond distances and angles within the coordination environment of each Ru(II) centre are otherwise unexceptional. The cation as a whole is reminiscent of a crown ether and has a chair-like conformation (Fig. 2(a)). The C(terpy)–O distances are shorter (C(23)–O(1) 1.354(5), C(8′)–O(5) 1.348(5) Å where C(8′) is related to C(8) by an inversion centre) than the remaining C–O bond distances in the polyethyleneoxy spacers (range 1.402(6)–1.444(5) Å). This, along with differences in C–O–C bond angles (Fig. 1 caption), is consistent with extension of π-delocalization from the aromatic ring to the first C–O bond of the spacer. The Ru · · · Ru separation across the macrocycle is 9.9 Å and this precludes any π-stacking interactions between the pair of symmetry-related pyridine rings that face one another across the cavity. The size of the macrocyclic cavity permits it to host one MeCN solvate molecule which is disordered over two positions with a 50 : 50 occupancy (Fig. 2(b)). The cavity is dumbbell shaped with the central constriction provided by the two {Ru(terpy)$_2$} motifs and it is not sensible to attempt to quantify the hole-size.

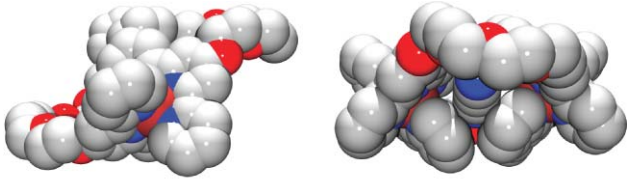

(a) (b)

Fig. 2 Space-filling diagrams of the cation in [Ru$_2$(**II**)$_2$][PF$_6$]$_4$·6MeCN showing (a) the chair-like conformation of the macrocycle and (b) the disordered solvent molecule that occupies the cavity in the macrocycle.

Single crystals of the compound [Ru$_2$(**III**)$_2$][PF$_6$]$_4$·2H$_2$O·MeCN were grown by the diffusion of diethyl ether vapour into an acetonitrile solution of the complex. Although the structure determined by X-ray diffraction is of relatively low quality, it confirms unambiguously that a [2 + 2] diruthenamacrocycle has been formed. Fig. 3 shows the structure of the [Ru$_2$(**III**)$_2$]$^{4+}$ cation and selected bond distances and angles are given in the caption. The structure of the complex cation is similar to that of [Ru$_2$(**II**)$_2$]$^{4+}$ and also exhibits a chair-like conformation. With the longer spacer, the macrocycle is expected to be larger and the Ru · · · Ru non-bonded distance is now 12.2 Å, and the cavity within the macrocycle is occupied by two, symmetry-related [PF$_6$]$^-$ ions. Once again, it is not useful to try to quantify the dimensions of the cavity, but subjectively two [PF$_6$]$^-$ ions are larger than the acetonitrile guests in [Ru$_2$(**II**)$_2$][PF$_6$]$_4$·6MeCN. The macrocyclic cations are arranged in rows along the crystallographic *b*-axis and interdigitation of spacer chains of adjacent molecules leads to short contacts in the range 3–3.5 Å between C and O atoms of adjacent chains. These chains are then stacked along the crystallographic *a*-axis (Fig. 4).

Formation of heteroleptic dimetallomacrocycles [Ru$_2$(I)(III)][PF$_6$]$_4$ and [Ru$_2$(II)(III)][PF$_6$]$_4$

After the success in the formation of the homoleptic [2 + 2] metallomacrocycles, we decided to explore the possibilities of preparing related heteroleptic complexes. We were successful in the syntheses of [Ru$_2$(**I**)(**III**)]$^{4+}$ and [Ru$_2$(**II**)(**III**)]$^{4+}$ (Fig. 5).

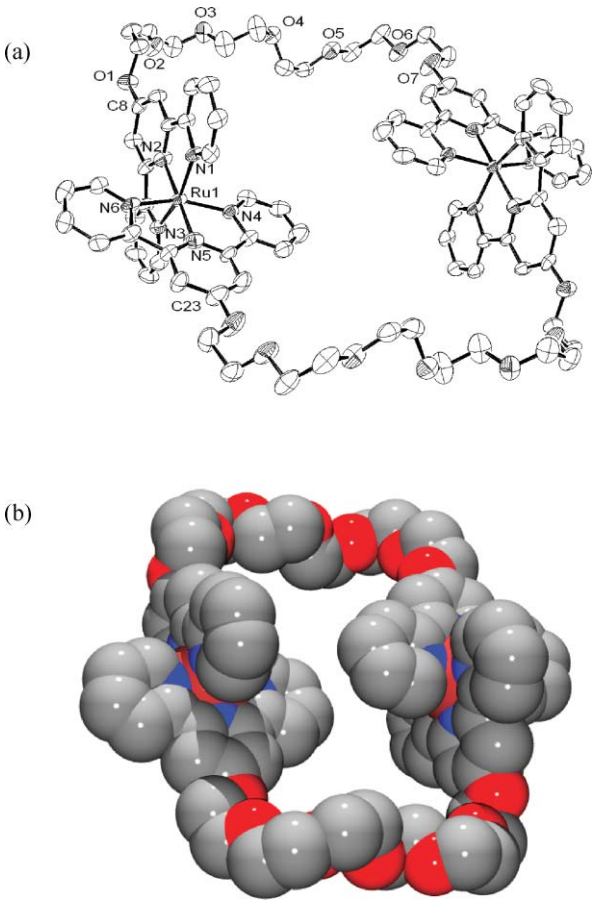

Fig. 3 (a) The molecular structure and atom labelling and (b) a space-filling diagram of the cation in [Ru$_2$(**III**)$_2$][PF$_6$]$_4$·2H$_2$O·CH$_3$CN. Hydrogen atoms are omitted for clarity. Atoms in the second half of the molecule are related to the first by inversion through a centre of symmetry. Selected bond lengths (Å) and angles (°): Ru(1)–N(1) 2.053(6), Ru(1)–N(2) 1.981(5), Ru(1)–N(3) 2.062(6), Ru(1)–N(4) 2.062(6), Ru(1)–N(5) 1.966(6), Ru(1)–N(6) 2.050(6), O(1)–C(8) 1.337(7), O(7)–C(23)′ 1.357(9); other C–O in the range 1.39(1)–1.43(1); N(1)–Ru(1)–N(2) 79.0(2), N(2)–Ru(1)–N(3) 78.6(2), N(4)–Ru(1)–N(5) 79.2(2), N(5)–Ru(1)–N(6) 78.5(2), C(8)–O(1)–C(31) 118.9(5), C(23′)–O(7)–C(42) 117.4(6), C(32)–O(2)–C(33) 111.7(5), C(34)–O(3)–C(35) 114.7(7), C(36)–O(4)–C(37) 112.9(7), C(38)–O(5)–C(39) 114.5(6).

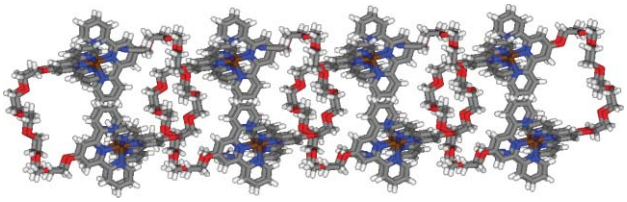

Fig. 4 Packing diagram for [Ru$_2$(**III**)$_2$][PF$_6$]$_4$·2H$_2$O·CH$_3$CN showing the arrangement of the complex cations and interdigitation of spacer chains of adjacent molecules.

However, all attempts to prepare [Ru$_2$(**I**)(**II**)]$^{4+}$, either by reaction of [Cl$_3$Ru(**I**)RuCl$_3$] with ligand **II**, or by treatment of [Cl$_3$Ru(**II**)RuCl$_3$] with ligand **I** under reducing conditions, gave very poor yields of mobile products. These reactions were therefore not pursued beyond trial studies.

The reaction of [Cl$_3$Ru(**I**)RuCl$_3$] with an equimolar quantity of **III** in the presence of *N*-ethylmorpholine in methanol yielded a red solution, indicative of the formation of a {Ru(terpy)$_2$}$^{2+}$ motif. However, it was noted that ≈30 mg of red precipitate formed in addition to the red solution. This material was insoluble in most solvents, including water and acetonitrile, and we believe it to be a random block copolymer. The insolubility

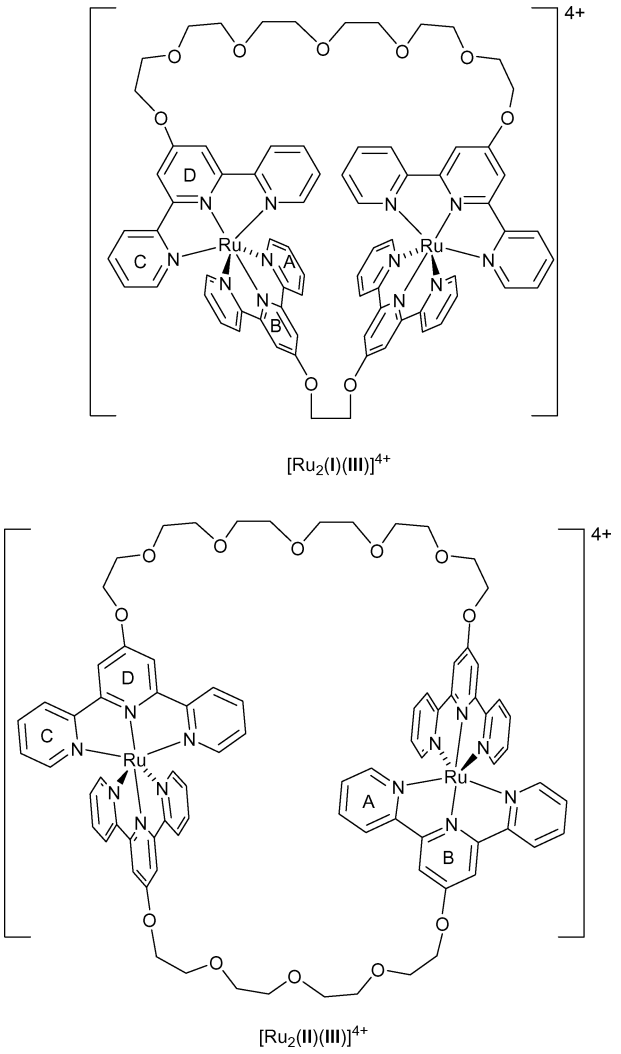

Fig. 5 Schematic representations of the structures of $[Ru_2(\mathbf{I})(\mathbf{III})]^{4+}$ and $[Ru_2(\mathbf{II})(\mathbf{III})]^{4+}$.

in water precludes formulation as a chloride salt of a higher nuclearity metallopolymer.[26] TLC analysis of the red solution showed that it contained a major component (R_f 0.4) along with some intractable baseline material. After filtering the insoluble material, the red solution was purified by column chromatography. The red fraction was treated with saturated aqueous NH_4PF_6 solution to precipitate the product as the hexafluorophosphate salt. This material was very soluble in MeCN solution, and exhibited peaks in its ESMS spectrum at m/z 1907 and 881 which were assigned to the molecular ions $[M - PF_6]^+$ and $[M - 2PF_6]^{2+}$, respectively. A peak at m/z 736 was tentatively assigned to $\{[(terpy)Ru(\mathbf{III})Ru][PF_6]_2\}^{2+}$ arising from cleavage of a ethyleneoxy linkage.

In the ^{1}H NMR spectrum of $[Ru_2(\mathbf{I})(\mathbf{III})][PF_6]_4$, two sets of terpyridine signals are observed, consistent with the formation of equivalent $[Ru(Xterpy)(Yterpy)]^{2+}$ motifs, where X and Y correspond to the polyethyleneoxy spacer units in each of ligands **I** or **III**. The terpy domains in the Xterpy and Yterpy ligands are chemically and magnetically non-equivalent. Furthermore, the signals for the methylene CH_2 signals are well resolved and their characteristic signatures generally resemble those of the free ligands **I** and **III**. A singlet is observed at δ 5.25 ppm and shows no coupling to any other methylene protons; this was confirmed in the ^{1}H–^{1}H COSY spectrum. This signal is therefore assigned to the four equivalent CH_2 protons of ligand **I**. In solution, relatively free rotation renders the potentially diastereotopic methylene protons of **I** in the complex equivalent, and a singlet is observed. Analysis of the ^{1}H–^{1}H NOESY spectrum of $[Ru_2(\mathbf{I})(\mathbf{III})][PF_6]_4$ (Fig. 6) shows a cross-peak between the δ 5.25 ppm singlet and a singlet at δ 8.38 ppm, which thus corresponds to the H_{3B} proton of the terpy subunit in ligand **I**. In addition, H_{3B} shows a cross-peak with the doublet at δ 7.89 ppm (H_{3A}), and further examination of the ^{1}H–^{1}H COSY spectrum allows the unequivocal assignment of protons H_{4A}, H_{5A} and H_{6A} in the subspectrum of ligand **I**. The other terpy subunit (corresponding to rings C and D of ligand **III**) are similarly assigned by a combination of NOESY and COSY spectra.

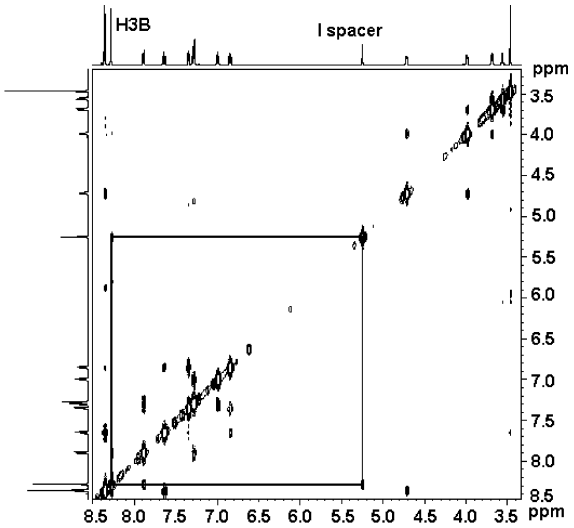

Fig. 6 The ^{1}H–^{1}H NOESY spectrum (500 MHz) of $[Ru_2(\mathbf{I})(\mathbf{III})][PF_6]_4$ in CD_3CN showing the cross-peak between H_{3B} and the methylene spacer of ligand **I**.

Formation and characterisation of $[Ru_2(II)(III)][PF_6]_4$

The reaction of equimolar quantities of ligand **II** and $[Cl_3Ru(\mathbf{III})RuCl_3]$ under the same conditions as that of **I** and $[Cl_3Ru(\mathbf{III})RuCl_3]$, followed by anion exchange, gave $[Ru_2(\mathbf{II})(\mathbf{III})][PF_6]_4$ in 45% yield. In contrast to the formation of $[Ru_2(\mathbf{I})(\mathbf{III})]^{4+}$, the reaction to generate $[Ru_2(\mathbf{II})(\mathbf{III})]^{4+}$ proceeded without competitive formation of insoluble (presumed polymeric) species, although the presence of intractable coloured species was evident during TLC analysis of the mixture. The desired product was easily separated from these materials by column chromatography, and was isolated as a red solid on reprecipitation as its hexafluorophosphate salt. The complex was characterised as $[Ru_2(\mathbf{II})(\mathbf{III})][PF_6]_4$ on the basis of elemental analysis, mass spectrometric data and NMR spectroscopy. Single crystals of the complex were obtained, but they diffracted too weakly to permit satisfactory data collection. The ESMS of the complex exhibited a peak envelope with isotopomers 0.5 mass units apart at m/z 947 which was assigned to $[M - 2PF_6]^{2+}$; the isotope distribution was an excellent match to that simulated for this ion.

The ^{1}H NMR spectrum of $[Ru_2(\mathbf{II})(\mathbf{III})][PF_6]_4$ was more difficult to interpret than that of $[Ru_2(\mathbf{I})(\mathbf{III})][PF_6]_4$. The cation $[Ru_2(\mathbf{II})(\mathbf{III})]^{4+}$ contains two rather similar ligands. Consequently, several signals for the terpy protons of the two ligands overlap, as do signals arising from ethyleneoxy units. This is particularly noticeable for the signals centred at δ 4.64 and 4.02 ppm which correspond to the CH_2 groups directly attached to the oxygen atom substituted at the 4′-positions of each terpy unit. The ^{1}H NMR spectrum of $[Ru_2(\mathbf{I})(\mathbf{III})][PF_6]_4$ was easily assigned due to the NOE interaction between the ethyleneoxy spacer singlet in ligand **I** and the H_3 protons on the central pyridine ring of the terpy in this ligand. The signals for the protons in the polyethyleneoxy chains in $[Ru_2(\mathbf{II})(\mathbf{III})]^{4+}$ cannot be assigned unambiguously, and therefore NOE interactions cannot be used

to assign individual terpy proton signals. By comparing the ^{1}H NMR spectrum of $[Ru_2(\mathbf{II})(\mathbf{III})]^{4+}$ with those of the macrocycles $[Ru_2(\mathbf{II})_2]^{4+}$, $[Ru_2(\mathbf{III})_2]^{4+}$ and $[Ru_2(\mathbf{I})(\mathbf{III})]^{4+}$ (Fig. 7) and with the aid of a ^{1}H–^{1}H-COSY experiment, these protons can be assigned with a reasonable degree of certainty (Table 1). The exceptions are protons H_{3B} and H_{3D} on the central terpy rings which cannot be resolved clearly.

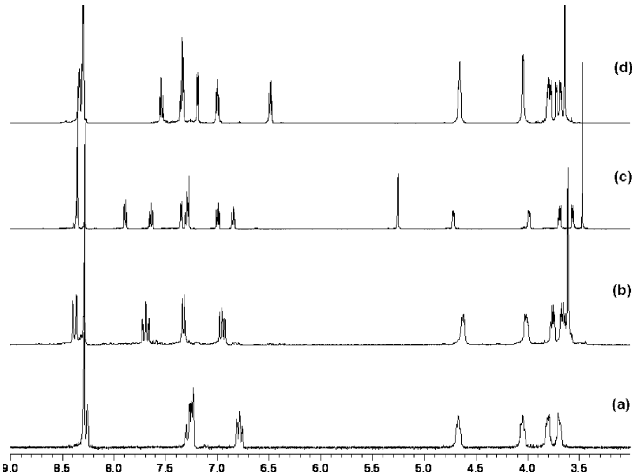

Fig. 7 The ^{1}H NMR spectra in CD_3CN of (a) $[Ru_2(\mathbf{II})_2][PF_6]_4$ (250 MHz) (b) $[Ru_2(\mathbf{III})_2][PF_6]_4$ (250 MHz), (c) $[Ru_2(\mathbf{I})(\mathbf{III})][PF_6]_4$ (500 MHz) and (d) $[Ru_2(\mathbf{II})(\mathbf{III})][PF_6]_4$ (500 MHz).

Comparisons of the chemical shift data for compounds $[Ru_2(\mathbf{II})_2][PF_6]_4$, $[Ru_2(\mathbf{III})_2][PF_6]_4$, $[Ru_2(\mathbf{I})(\mathbf{III})][PF_6]_4$ and $[Ru_2(\mathbf{II})(\mathbf{III})][PF_6]_4$ with the mononuclear complex $[Ru(EtOterpy)_2][PF_6]_2$[27] (EtOterpy = 4′-ethoxy-2,2′:6′,2″-terpyridine) and the linear coordination polymer $\{Ru[terpy(OCH_2CH_2)_2Oterpy][BF_4]_2\}_n$[9] (terpy$(OCH_2CH_2)_2$Oterpy = 1,5-bis(2,2′:6′,2″-terpyridin-4′-yloxy)-3-oxapentane) show significant differences in the chemical shifts of the terpy protons. These differences (Table 2) are most pronounced for protons H_{3A}, H_{4A} and H_{5A}. These protons are most affected by shielding in the metallomacrocycles as they are directed towards the interior of the macrocyclic cavity. The largest chemical shift differences are observed on going from the linear polymer to $[Ru_2(\mathbf{I})(\mathbf{III})]^{4+}$ and $[Ru_2(\mathbf{II})(\mathbf{III})]^{4+}$ (Table 2). In $[Ru_2(\mathbf{I})(\mathbf{III})]^{4+}$, the short spacer in **I** forces the pair of terpy motifs closer together than in the other macrocyclic complexes, giving rise to larger $\Delta\delta$ values. In contrast, the largest macrocyclic cavity is in $[Ru_2(\mathbf{III})_2]^{4+}$, and consistent with this, Table 2 reveals the smallest $\Delta\delta$ values. Protons H_{3A} and H_{4A} are most perturbed in $[Ru_2(\mathbf{I})(\mathbf{III})]^{4+}$, whereas in $[Ru_2(\mathbf{II})_2]^{4+}$ and $[Ru_2(\mathbf{II})(\mathbf{III})]^{4+}$, protons H_{4A} and H_{5A} show the greatest chemical shift change. The short spacer in ligand **I** forces the two terpy motifs in this ligand to adopt a strained V-shape in $[Ru_2(\mathbf{I})(\mathbf{III})]^{4+}$, forcing the H_{3A} protons into the macrocyclic cavity and lowering the effect of shielding on H_{5A}. In contrast, the longer spacers in $[Ru_2(\mathbf{II})_2]^{4+}$ and $[Ru_2(\mathbf{II})(\mathbf{III})]^{4+}$ allow the terpy motifs to adopt a less strained arrangement in the complex, with the pairs of terpy motifs on each ligand being more or less parallel to each other. This orients protons H_{4A} and H_{5A}, in particular towards the cavity of the macrocycle resulting in their greater perturbation from the linear situation at the expense of H_{3A}.

Metallopolymer formation during the cyclisation process

Formation of the metallomacrocycles discussed in this paper occurs through a two-step process. The first is the formation of the diruthenium(III) chloride adduct of one of the ligands and the second is the reaction of this species with a stoichiometric amount of a second ligand under reducing conditions. This strategy is the same as that used by Newkome and co-workers who reported a 43% yield of a [6 + 6] metallomacrocyclic hexagonal species from the reaction of ligand **IV** (Chart 1) and its diruthenium(III) chloride adduct.[3] In this case, the angle subtended by the terpy subunits in ligand **IV** preorganises the system for the formation of a hexamer. However, the moderate yield suggests that the formation of other species in addition to the isolated product occurs, resulting in the need for chromatographic purification of the metallomacrocycle. While the nature of the other species has not been discussed, it is likely that oligomers or metallopolymeric material resulted from the uncontrolled assembly of the two components.

The formation of ruthenium(II) metallopolymers from bis(terpyridine) ligands has been well documented.[8–12,28] In most cases, these species are formed when the spacer region connecting the terpy subunits is rigid.[28,29] However, recent work by Schubert and co-workers has focused on the formation and characterisation of ruthenium(II) metallopolymers from bis(terpyridine) ligands connected through flexible spacer units.

Table 1 Chemical shift data (δ (ppm)) for the ruthenamacrocycles $[Ru_2(\mathbf{II})_2][PF_6]_4$, $[Ru_2(\mathbf{III})_2][PF_6]_4$, $[Ru_2(\mathbf{I})(\mathbf{III})][PF_6]_4$, $[Ru_2(\mathbf{II})(\mathbf{III})][PF_6]_4$ and some reference compounds in CD_3CN solution

Complex	H_{6A}	H_{5A}	H_{4A}	H_{3A}	H_{3B}	H_{6C}	H_{5C}	H_{4C}	H_{3C}	H_{3D}
$[Ru_2(\mathbf{II})_2][PF_6]_4$	7.24	6.78	7.27	8.26	8.29					
$[Ru_2(\mathbf{III})_2][PF_6]_4$	7.32	6.95	7.69	8.37	8.29					
$[Ru_2(\mathbf{I})(\mathbf{III})][PF_6]_4$	7.28	6.99	7.29	7.89	8.28	7.35	6.85	7.64	8.36	8.35
$[Ru_2(\mathbf{II})(\mathbf{III})][PF_6]_4$	7.31	6.47	7.32	8.29	8.277	7.17	6.98	7.52	8.32	8.277
$[Ru(EtOtpy)_2][PF_6]_2$[a]	7.37	7.13	7.88	8.46	8.27					
$\{Ru[terpy(OCH_2CH_2)_2Oterpy][BF_4]_2\}_n$[b]	7.41	7.18	7.92	8.50	8.37					

[a] Ref. 27. [b] Ref. 9.

Table 2 Chemical shift differences ($\Delta\delta$ (ppm)) between $[Ru_2(\mathbf{II})_2][PF_6]_4$, $[Ru_2(\mathbf{III})_2][PF_6]_4$, $[Ru_2(\mathbf{I})(\mathbf{III})][PF_6]_4$ and $[Ru_2(\mathbf{II})(\mathbf{III})][PF_6]_4$ and the linear polymer $\{Ru[tpy(OCH_2CH_2)_2Otpy][BF_4]_2\}_n$,[5b] where $\Delta\delta = \delta_{\text{linear}} - \delta_{\text{cyclic}}$[a]

Complex	H_{6A}	H_{5A}	H_{4A}	H_{3A}	H_{3B}	H_{6C}	H_{5C}	H_{4C}	H_{3C}	H_{3D}
$[Ru_2(\mathbf{II})_2][PF_6]_4$	0.17	0.40	0.65	0.24	0.08					
$[Ru_2(\mathbf{III})_2][PF_6]_4$	0.09	0.23	0.23	0.13	0.08					
$[Ru_2(\mathbf{I})(\mathbf{III})][PF_6]_4$	0.13	0.19	0.63	0.61	0.09	0.06	0.33	0.28	0.14	0.02
$[Ru_2(\mathbf{II})(\mathbf{III})][PF_6]_4$	0.10	0.71	0.60	0.21	0.09	0.24	0.20	0.40	0.18	0.09

[a] In CD_3CN solution.

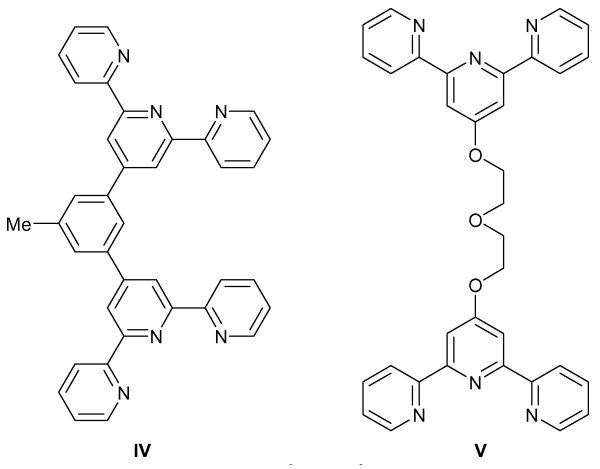

Chart 1 Structures of ligands **IV**[3] and **V**.[9]

Reaction of ligand **V** (an analogue of ligands **I**, **II** and **III**) (Chart 1) with $[Ru(CH_3COCH_3)_6][BF_4]_3$ in ethanol afforded a linear metallopolymer in near quantitative yield.[9]

The complexes $[Ru_2(\mathbf{II})_2][PF_6]_4$, $[Ru_2(\mathbf{III})_2][PF_6]_4$, $[Ru_2(\mathbf{I})(\mathbf{III})][PF_6]_4$ and $[Ru_2(\mathbf{II})(\mathbf{III})][PF_6]_4$ were formed in yields of 35, 32, 13 and 45%, respectively. During their syntheses, other species were observed. TLC analysis of the crude reaction mixtures showed the presence of orange/red species of low mobility. These species are likely to be higher oligomers or metallopolymers, which have been observed in the self-assembly of polynuclear iron(II) metallocycles with analogous bis(terpyridine) ligands.[4,26] Significantly, the lowest yield is for the formation of $[Ru_2(\mathbf{I})(\mathbf{III})][PF_6]_4$, and corresponds to the presence of the shortest spacer (in ligand **I**) where linear polymer formation is likely to be preferred over the assembly of a metallomacrocycle. We believe that the insoluble red precipitate formed during the reaction is such as polymer. Interestingly, attempts to form $[Ru_2(\mathbf{I})(\mathbf{III})]^{4+}$ by the reaction of terpy$(OCH_2CH_2)_2$Oterpy $[Cl_3Ru(\mathbf{III})RuCl_3]$ with ligand **I** (rather than $[Cl_3Ru(\mathbf{I})RuCl_3]$ with **III** as described earlier) failed to give any of the desired macrocyclic complex.

A comparison of our results with those of Newkome,[3] indicate that the yields of metallomacrocycles $[Ru_2(\mathbf{II})_2][PF_6]_4$, $[Ru_2(\mathbf{III})_2][PF_6]_4$, $[Ru_2(\mathbf{I})(\mathbf{III})][PF_6]_4$ and $[Ru_2(\mathbf{II})(\mathbf{III})][PF_6]_4$ are reasonable in the light of the flexible nature of the spacer units which have a significant potential for metallopolymer formation. Preliminary gas phase molecular modelling studies (MM2) suggest that the terpy motifs in ligands **II** and **III** are able to interact through π-stacking, and this may provide sufficient preorganisation to encourage the formation of macrocyclic rather than polymeric species.

Conclusions

We have shown that ditopic ligands containing two terpy metal-binding domains separated by flexible, but possibly preorganised, polyethyleneoxy spacers form [2 + 2] metallomacrocycles with ruthenium(II). This is in contrast to the behaviour with labile iron(II) salts, which yield metallomacrocycles of various nuclearity. Varying amounts of metallopolymer are also formed but are readily separated from the molecular species. We believe that the driving force for the formation of the metallomacrocyclic species is entropic.

Acknowledgements

We thank the Swiss National Science Foundation and the University of Basel for financial support. We also thank Dr Klaus Külicke (University of Basel) for assistance with 2D-NMR spectroscopy and Sebastien Reymann for recording some of the mass spectra.

References

1 E. C. Constable and E. Schofield, *Chem. Commun.*, 1998, 403.
2 G. U. Priimov, P. Moore, P. K. Maritim, P. K. Butalanyi and N. W. Alcock, *J. Chem. Soc., Dalton Trans.*, 2000, 445.
3 G. R. Newkome, T. J. Cho, C. N. Moorefield, G. R. Baker, R. Cush and P. S. Russo, *Angew. Chem., Int. Ed.*, 1999, **38**, 3717; G. R. Newkome, T. J. Cho, C. N. Moorefield, R. Cush, P. S. Russo, L. A. Godínez, M. J. Saunders and P. Mohapatra, *Chem. Eur. J.*, 2002, **8**, 2946; G. R. Newkome, T. J. Cho and C. N. Moorefield, *Chem. Commun.*, 2002, 2164; P. Wang, C. N. Moorefield and G. R. Newkome, *Org. Lett.*, 2004, **6**, 1197; G. R. Newkome, T. J. Cho, C. N. Moorefield, P. P. Mohapatra and L. A. Godínez, *Chem. Eur. J.*, 2004, **10**, 1493.
4 C. B. Smith, E. C. Constable, C. E. Housecroft and B. M. Kariuki, *Chem. Commun.*, 2002, 2068.
5 E. C. Constable, C. E. Housecroft and C. B. Smith, *Inorg. Chem. Commun.*, 2003, **6**, 1011.
6 H. S. Chow, E. C. Constable, C. E. Housecroft and M. Neuburger, *Dalton Trans.*, 2003, 4568.
7 E. C. Constable, C. E. Housecroft, M. Neuburger, S. Schaffner and E. J. Shardlow, *Dalton Trans.*, 2005, 234.
8 U. S. Schubert, C. Eschbaumer, O. Hein and P. R. Andres, *Tetrahedron Lett.*, 2001, **42**, 4705.
9 H. Hofmeier, S. Schmatloch, D. Wouters and U. S. Schubert, *Macromol. Chem. Phys.*, 2003, **204**, 2197.
10 S. Schmatloch, M. Fernández González and U. S. Schubert, *Macromol. Rapid Commun.*, 2002, **23**, 957.
11 H. Hofmeier and U. S. Schubert, *Chem. Soc. Rev.*, 2004, **33**, 373.
12 P. R. Andres and U. S. Schubert, *Adv. Mater.*, 2004, **16**, 1043.
13 M. Fujita, J. Y. Kwon, S. Washizu and K. Ogura, *J. Am. Chem. Soc.*, 1994, **116**, 1151.
14 H. Piotrowski, K. Polborn, G. Hilt and K. Severin, *J. Am. Chem. Soc.*, 2001, **123**, 2699.
15 K. Severin, *Coord. Chem. Rev.*, 2003, **245**, 3; M. J. Rauterkus and B. Krebs, *Angew. Chem., Int. Ed.*, 2004, **43**, 1300; H. Piotrowski and K. Severin, *Proc. Natl. Acad. Sci. USA*, 2002, **99**, 4997; M. Fujita, J. Yazaki and K. Ogura, *J. Am. Chem. Soc.*, 1990, **112**, 5645; J. Stang and K. Chen, *J. Am. Chem. Soc.*, 1995, **117**, 1667.
16 J. J. Bodwin and V. L. Pecoraro, *Inorg. Chem.*, 2000, **39**, 3434; M. Moon, I. Kim and M. S. Lah, *Inorg. Chem.*, 2000, **39**, 2710; M. S. Lah and V. L. Pecoraro, *J. Am. Chem. Soc.*, 1989, **111**, 7258; V. L. Pecoraro, A. J. Stemmler, B. R. Gibney, J. J. Bodwin, H. Wang, J. W. Kampf and A. Barwinski, *Prog. Inorg. Chem.*, 1997, **45**, 83; J. J. Bodwin, A. D. Cutland, R. G. Malkani and V. L. Pecoraro, *Coord. Chem. Rev.*, 2001, **216–217**, 489.
17 R. W. Saalfrank, N. Löw, F. Hampel and H.-D. Stachel, *Angew. Chem., Int. Ed.*, 1996, **35**, 2209; C. Dendrinou-Samara, G. Psomas, L. Iordanidis, V. Tangoulis and D. P. Kessissoglou, *Chem. Eur. J.*, 2001, **7**, 5041; C. Dendrinou-Samara, M. Alexiou, C. M. Zaleski, J. W. Kampf, M. L. Kirk, D. P. Kessissoglou and V. L. Pecoraro, *Angew. Chem., Int. Ed.*, 2003, **42**, 3763; J. A. Johnson, J. W. Kampf and V. L. Pecoraro, *Angew. Chem., Int. Ed.*, 2003, **42**, 546; B. R. Gibney, A. J. Stemmler, S. Pilotek, J. W. Kampf and V. L. Pecoraro, *Inorg. Chem.*, 1993, **32**, 6008; A. Caneschi, A. Cornia and S. J. Lippard, *Angew. Chem., Int. Ed.*, 1995, **34**, 467; B. Kwak, H. Rhee, S. Park and M. S. Lah, *Inorg. Chem.*, 1998, **37**, 3599; A. J. Blake, R. O. Gould, C. M. Grant, P. E. Y. Milne, D. Reed and R. E. P. Winpenny, *Angew. Chem., Int. Ed.*, 1994, **33**, 195; H. Saarinen and M. Orama, *Acta Chem. Scand*, 1998, **52**, 1209; C. Dendrinou-Samara, C. M. Zaleski, A. Evagorou, J. W. Kampf, V. L. Pecoraro and D. P. Kessissoglou, *Chem. Commun.*, 2003, 2668; S.-X. Liu, S. Lin, B.-Z. Lin, C.-C. Lin and J.-Q. Huang, *Angew. Chem., Int. Ed.*, 2001, **40**, 1084; R. W. Saalfrank, N. Löw, S. Kareth, V. Seitz, F. Hampel, D. Stalke and M. Teichert, *Angew. Chem., Int. Ed.*, 1998, **37**, 172.
18 W. L. F. Armarego and D. D. Perrin, *Purification of Laboratory Chemicals*, Butterworth-Heinemann, Oxford, UK, 4th edn., 1996.
19 E. C. Constable and M. D. Ward, *J. Chem. Soc., Dalton Trans.*, 1990, 1405.
20 *COLLECT Software*, Nonius BV, 1997–2001.
21 A. Altomare, G. Cascarano, G. Giacovazzo, A. Guagliardi, M. C. Burla, G. Polidori and M. Camalli, *J. Appl. Crystallogr.*, 1994, **27**, 435.
22 D. J. Watkin, C. K. Prout, J. R. Carruthers, P. W. Betteridge and R. I. Cooper, *CRYSTALS*, Issue 11, Chemical Crystallography Laboratory, Oxford, UK, 2001.
23 E. C. Constable, C. E. Housecroft, M. Cattalini and D. Phillips, *New J. Chem.*, 1998, 193.

24 E. C. Constable and D. Phillips, *Chem. Commun.*, 1997, 827.
25 See, for example:E. C. Constable and A. M. W. Cargill Thompson, *J. Chem. Soc., Dalton Trans.*, 1994, 1409; E. C. Constable and P. Harverson, *Polyhedron*, 1999, **18**, 3093; E. C. Constable and A. M. W. Cargill Thompson, *New J. Chem.*, 1992, 855; M. Beley, J. P. Collin, R. Louis, B. Metz and J.-P. Sauvage, *J. Am. Chem. Soc.*, 1991, **113**, 8521; S. Weidner and Z. Pikramenou, *Chem. Commun.*, 1998, 1473.
26 E. C. Constable, C. E. Housecroft and C. B. Smith, unpublished results.
27 M. Maestri, N. Armaroli, V. Balzani, E. C. Constable and A. M. W. Cargill Thompson, *Inorg. Chem.*, 1995, **34**, 2759.
28 S. Kelch and M. Rehahn, *Macromolecules*, 1999, **32**, 5818.
29 J. Hjelm, E. C. Constable, E. Figgemeier, A. Hagfeldt, R. Handel, C. E. Housecroft, E. Mukhtar and E. Schofield, *Chem. Commun.*, 2002, 284.